

Computer Modeling of Time-of-Flight Scintillator Pulses

Jason Aftosmis, John Ficenec,
David Jenkins, and Elton Smith
24 August, 1996

1 INTRODUCTION

It is the purpose of this study to investigate, by a computer modeling of pulses in Time-of-Flight (TOF) detectors, the behavior of the leading-edge of scintillator pulses subject to varying conditions and, ultimately, investigate the corresponding time-walk corrections. The shape of the pulse is generated by histogramming Monte-Carlo data generated by the CERN program Guide7¹. That histogram is convoluted with a Gaussian response function to simulate the time-spread of the photomultiplier tube (PMT), and the cable and electronics dispersion. This convoluted pulse is input to a *Mathematica* routine which calculates the different time-walk plots and allows graphical comparison of fits to these plots.

2 INPUT PARAMETERS

The Guide7 program allows a number of ways to adjust the conditions in order to realistically simulate the pulses in plastic scintillators. These parameters (with their corresponding nominal values or figure references in parentheses) include:

- the geometry of the scintillator (see Fig. 1)
- the geometry of the light guide and PMT setup (see Fig. 2)
- the geometry of the particle path through the scintillator (assumed to be perpendicular to the scintillator surface)(see Fig. 3).
- the indices of refraction for the various materials (scintillator, 1.58; light guide, 1.49)
- the speed of the particle through the scintillator (0.9c)

¹ Guide7 handbook: CERN Library 76-21

- the nature of the end most distant from the PMT (black, no reflection).
- the scintillator decay-time (2.3 ns)
- the scintillator attenuation length
- the maximum time-delay of accepted events (199 ns)

The run-time of the program is determined by the input values of the number of generated photons for a given path and the number of accepted photons for that path, of which it chooses the least in the decision of the program end. Added to the Guide7 program was a routine which calculated an additional time-delay to account for different transit-times through the PMT as a function of the position of the photon on the photocathode. We used photo-electron transit-time data illustrated in Figs. 4 and 5 and parameterized it as a function of the distance from the cathode center. There are additional assumptions of no loss of light upon reflection and a uniform PMT conversion sensitivity over the face of the photocathode.

In the detector geometry, as defined in the Guide7 program, the coordinate convention is such that points along the scintillator length (the z-axis) are negative positions with respect to the z-axis origin at the interface between the scintillator and light guide. The light guide and PMT are then of positive position along this z-axis. The cross-section of the detector in the x,y-plane is centered about (0,0) (See Fig. 1 and 2).

3 METHOD OF CALCULATION

3.1 The CERN Guide7 Program

The Guide7 program is a Monte-Carlo simulation which was created particularly for this sort of study. After reading an input file containing the aforementioned parameters, the program chooses randomly a point on the particle path and calculates the time-delay due to its position along the path using the particle velocity. A random direction (in the hemisphere toward the single PMT) is then chosen for the photon and another time-delay is calculated based on the time-delay distribution of scintillation light defined by input decay constants. This photon is then tracked by extrapolating the direction vector to all of its intersections with defined planes. The closest intersection is calculated and it is determined whether, based on the critical angle, reflection is to take place. If the photon reflection occurs, characteristics of the photon reflection, such as direction and intensity (loss of light on reflection), are calculated. The direction vector is extrapolated again and the reflections are analyzed, until an extrapolation yields intersection with a plane which is defined as the gate. We have written a supplemental routine which is now called

to calculate a time-delay due to the position of photons incident on the PMT according to the included plots (Figs. 4,5). Throughout these extrapolations, interesting quantities such as distance traveled, time, number of reflections and intensity are stored, whereupon incidence on a gate determines whether or not the photon is to be accepted. If the photon is accepted, relevant quantities are output to a file (time in this case). The parameters which determine program run-time are checked, and if still satisfied, another photon is tracked. That is, another random point is chosen on the particle path associated with a random direction and a randomly chosen time according to the scintillation decay distribution, and the extrapolation of the photon direction vector ensues.

There are many components which contribute to the time distribution. The first time-component is calculated according to the random position along the particle path at which the photon is emitted. Then we calculate the delay-time of the photon corresponding to its random assignment in the scintillation decay distribution (of the form: $A_1 \text{Exp}(-t/A_2)$). Then, according to its total track distance through the plastic scintillator and light guide, another appropriate time component is added. Finally, another time quantity is added with respect to the position at which the photons strike the photomultiplier face.

3.2 Pulse Histogram Convolution

To simulate additional spreading in the PMT (electron projection time and electronic response time) and cable dispersion, we fold an additional time-delay according to a Gaussian distribution. Once Guide7 has generated the data in a file, that file is read by a separate FORTRAN program, Hconv, specifically written for the folding in this study. The program uses a number of HBOOK² commands in its construction of the histograms. Those histograms consisting of the raw Guide7 data are saved, and can be viewed by PAW++³ at this time, but those histograms are also unpacked into arrays upon which the Hconv program performs a convolution. It does so by first defining a response function (a Gaussian of definable width) and then calling four other subroutines, convlv.f, fourl.f, realft.f, twofft.f⁴, containing the Fast Fourier Transform (FFT) algorithm. The Hconv program, after the transform has been executed, then packs the convoluted array into a histogram. At this point, an HBOOK command is used to determine the integral of the histograms so that the areas can be used to rescale the histogram in the interest of keeping the pulse histogram area constant throughout the convolution. The program proceeds to pack the rescaled, convoluted pulse into a histogram for viewing as well as

² CERN Program Library Long Writeup Y250, Version 4.21

³ Physics Analysis Workstation, CERN Program Library Long Writeup Q121

⁴ Press, William H., Numerical Recipes, 1st ed. (Cambridge Univ. Press, New York, 1986), pp. 397-413

output the final array into an ASCII file which is read by the *Mathematica* program.

3.3 Time-Walk Calculation

After the convoluted histogram array is read by *Mathematica*, the two coordinates being time and the respective pulse height, we take only the data which defines the leading-edge (the *Mathematica* representation of the pulse is shown in Fig. 6). This must be done by careful inspection since the FFT algorithm is not free from aliasing. That data array is then transformed so as to make the time a function of amplitude. From that array, a different set of data arrays is created where each array in the set has its pulse-height coordinates scaled by a constant k . That constant k is iterated from 0.2 (20% of the pulse) to unity in steps of 0.025 so that each of the data arrays in the set corresponds to differently sized pulses for a given pulse shape. Interpolating functions are generated to fit each data array and each of these functions is evaluated at the trigger threshold giving a triggering-time. Then another array is made; its coordinates being the iterated constant k used to scale the pulse amplitude and the triggering-time, respectively. This data can then be plotted to show the dependence of triggering-time on the pulse-height and one can fit a function to compare with other time-walk correction curves. With the ability now to study the time-walk correction for different magnitudes of a given pulse shape, we can investigate how the time-walk correction plots compare for the variety of pulse shapes generated by Guide7.

4 EFFECTS ON PULSE SHAPES

Following are summaries of results from the investigation of the input parameter effects on the pulse shapes.

4.1 A Point Source Near the Phototube

To examine the effect of different source particle path geometries, pulses (histograms) were generated for a point source at the center of the scintillator cross-section at 0.1 cm into the scintillator end closest to the PMT. As we see in the unconvoluted pulse-histogram (Fig. 7), the rise-time was extremely short and, having eliminated time-spread due to position along particle path and virtually eliminated any time difference due to varying track length, only the time-delay due to position on PMT face and scintillation-decay-time are factors in the pulse shape. The tail of the pulse decays according to the parameters of the scintillator response function and the extremely short rise-time can be attributed to the limiting of the time-spreads.

4.2 Line Sources through the Edge and Center

It is also of great interest to compare the resultant pulse shapes of particle paths through the center and edge of the scintillator (Fig. 3). It was found that the pulse shapes did not differ by any great amount as one can see by the unconvoluted and overlaid histograms (Fig. 8). The leading-edges are however not identical, due to the different light-source-path time-spreads, and a discussion of the time-walk correction curve follows. It is worth noting that both paths were run for the same number of events so the edge pulse, which would experimentally be smaller, is the same magnitude as the center source path pulse.

4.3 Effect of Varying Source Position

The effect of the position of the particle path along the scintillator is manifested in the pulse shape. For sources most distant from the PMT, there is a possibility of more reflections which, in turn, produces a greater spread of photon track length and corresponding time-delay. Thus there is longer rise-time as one gets increasingly farther from the PMT and, as we shall see, this is visible in the time-walk correction curves compared among the varying source positions. In Fig. 9, one can see the sequence of pulses generated by line sources through the center of the scintillator at -57 cm, -114 cm, -229 cm, and -286 cm with respect to the previously defined geometry.

4.4 Time Response of Phototube and Cable

The intrinsic response of the PMT to a single photo-electron is approximately a Gaussian with a full-width-half-maximum (FWHM) of 0.425 ns ($\sigma = 1$ ns).⁵ However, after 400 ns of RG-213 delay cable, the rise-time deteriorates to approximately 4.2 ns which roughly corresponds to a convolution with a Gaussian with a FWHM of 3.5 ns. Thus far we have convoluted so that a pulse from a light source at -172 cm with the center path line geometry would have a rise-time (10-90%) of about 4.2 ns using a Gaussian with FWHM of 3.5 ns. Then varying the response of the PMT and the cable dispersion, by convoluting the pulse shape in different amounts, would affect the leading-edge. Histograms of a pulse convoluted by a Gaussian with FWHMs of 2.5 ns, 3.5 ns, and 4.5 ns are shown overlaid in Fig.10 and show the pulse-shape dependence on the response function.

4.5 Scintillation Decay Time Constant

The response of the TOF detector changes for different scintillation-decay-time constants (SDTC). We checked this effect on the pulse shape for three values of the SDTC (1.6 ns, 2.3 ns and 3.0 ns) for a center-geometry, line-pulse at -172 cm.

⁵ L.G. Hyman, R.M. Schwarcz, R.A. Schluter, Rev. Sci. Inst. **35**, 393 (1964).
L.G. Hyman, Rev. Sci. Inst. **36**, 193 (1965).

Fig. 11 shows that the pulse-shape and leading-edge dependence on the SDTC. The smaller SDTC corresponds to a smaller rise-time.

5 TIME-WALK CORRECTION

As a standard for comparison, unless otherwise noted, a pulse whose light source was a center path at -172 cm convoluted with a Gaussian of 3.5 ns FWHM is used in the discussion. Exclusive of the trigger threshold comparison discussion, a discriminator threshold of 2% of the maximum pulse amplitude is used in the time-walk correction calculation.

5.1 Correction Plots Varying Source Position

Since we have seen that the leading-edge shape changes with a change in the distance of the source particle path from the PMT, we would also expect that the time-walk correction curve would be dependent on the position of the particle path. Plots for comparison, where the curves have been vertically adjusted to show more clearly the difference in shape, were made for seven points along the scintillator using a triggering level of 2% (Figs. 12,13). One can see that the more distant pulse sources, having a less steep leading-edge, have a time-walk correction curve which is more steep. The difference in time-walk correction for pulses at different positions are on the order of tenths of nanoseconds over the range of pulse amplitudes.

In all time-walk discussions, two plots were made for each section and are presented in pairs. The uppermost of the pair shows the curves with a time-scale corresponding to the pulse time. The lower plot has the same curves from the same calculation but, to show more clearly the difference in curve shape, the plots have been adjusted vertically, making the vertical-axis time-scale only relative.

5.2 Correction Plots Varying Convolution

Similarly, the amount by which we convolute the raw pulse to mimic the effect of PMT-rise-time and cable dispersion, also changes the time-walk correction curve. One can see in Figs. 14,15 that the curves differ in shape enough that over the domain, the shape difference could yield time-walk correction differences as great as tenths of nanoseconds.

5.3 Correction Plots Varying Discriminator Threshold

The time-walk correction curve for a given pulse is also somewhat dependent on the trigger-pulse-height-discriminator level that one uses in the calculation. Using trigger-heights from 0.99% to 3.97% in steps of about 0.60%, we have generated overlain time-walk correction curves for each trigger height (Figs. 16,17). It can be seen that the shape differs enough that the corrections can differ on the order of tenths of nanoseconds for these trigger heights on this domain of pulse amplitude

from 20% to full pulse.

5.4 Correction Plots of Edge and Center Paths

The shapes of the pulses from the edge and center source particle paths, though different only slightly in Figs. 18,19, also yield time-walk correction curves with distinct shapes. The edge path has a slightly more shallow curve than the center path pulse. This difference in shape yields a time-walk correction which can be on the order of hundredths of nanoseconds over the relative pulse amplitude domain.

5.5 Correction Plots Varying SDTC

Time-walk correction curves for the pulse where the SDTC has been varied also differ. Their shapes are different enough that, among the values investigated, the time-walk can differ as much as tenths of nanoseconds as Figs. 20,21 show. The pulses with the greater SDTC's have greater time-walk correction.

6 SUMMARY

Having modeled the TOF detector pulse using the Guide7 program, it is clear that the pulse shapes are sensitive to many conditions which vary in the experiment. The position of the particle in scintillator, energy deposited (pulse height), electronic response and cable dispersion (convolution), discriminator threshold and scintillation-decay-time-constant affect the time-walk correction on the order of tenths of nanoseconds. Likewise, the time-walk correction curve for selected edge and center light source geometries differ on the order of hundredths of nanoseconds. By studying these effects using computer modeling, as we have done, one can investigate which conditions and effects are significant in the timing and, in turn, develop better timing techniques.

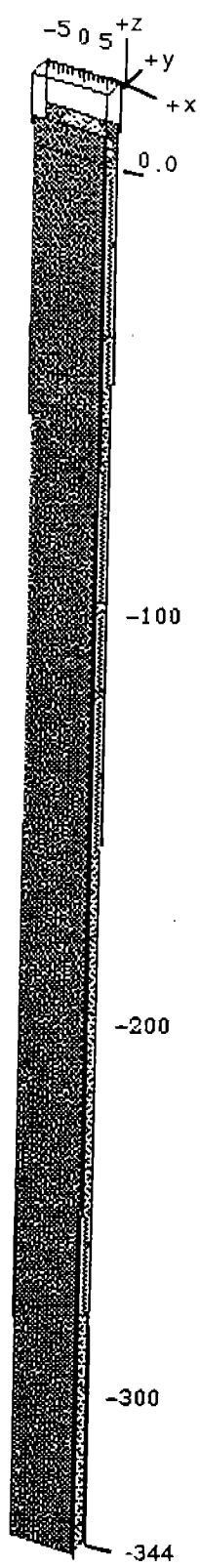


Figure 1:
The TOF detector as defined in Guide7

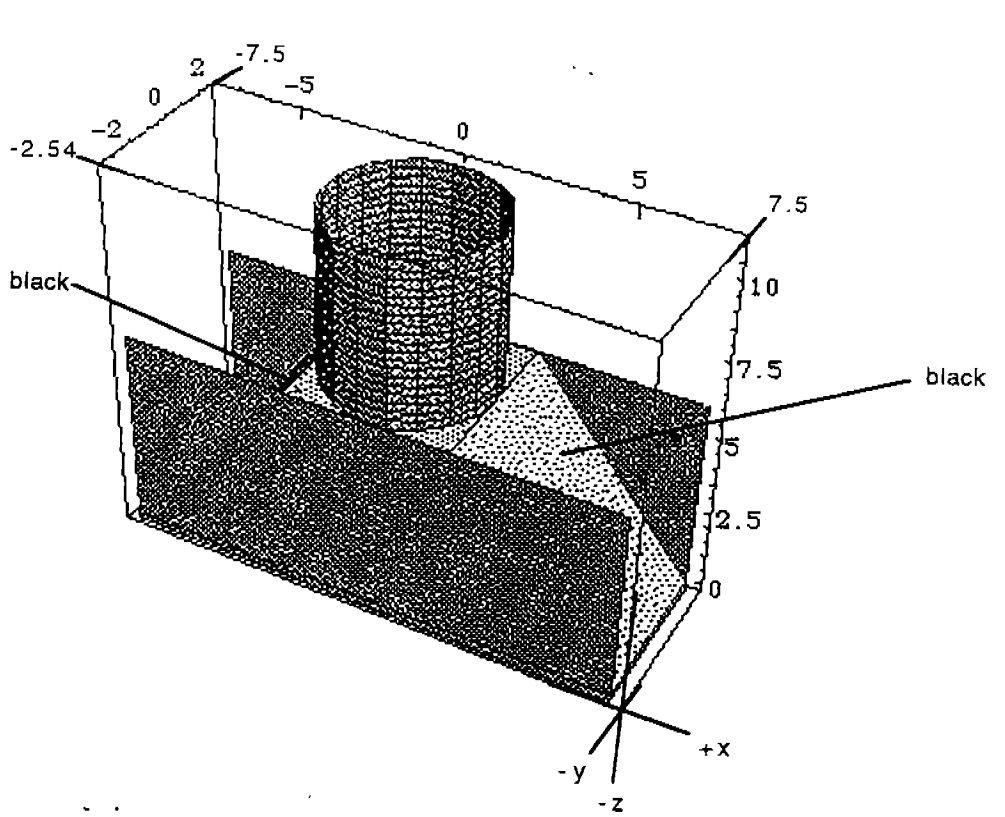


Figure 2:
The TOF light guide with PMT as defined in Guide7 using solid planes. The two planes labeled as 'black' have been blackened in the plane definition.

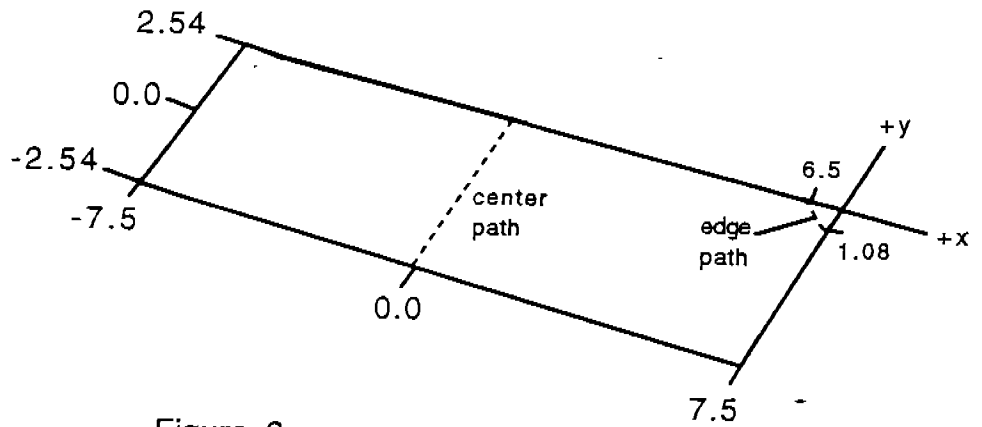


Figure 3:
A cross section of the TOF scintillator showing the geometry of the center and edge source particle paths

Note: All units are centimeters.

EMI-9954A 'X' SCAN AMPLITUDE & RELATIVE TIME SHIFT
@ 2000 V

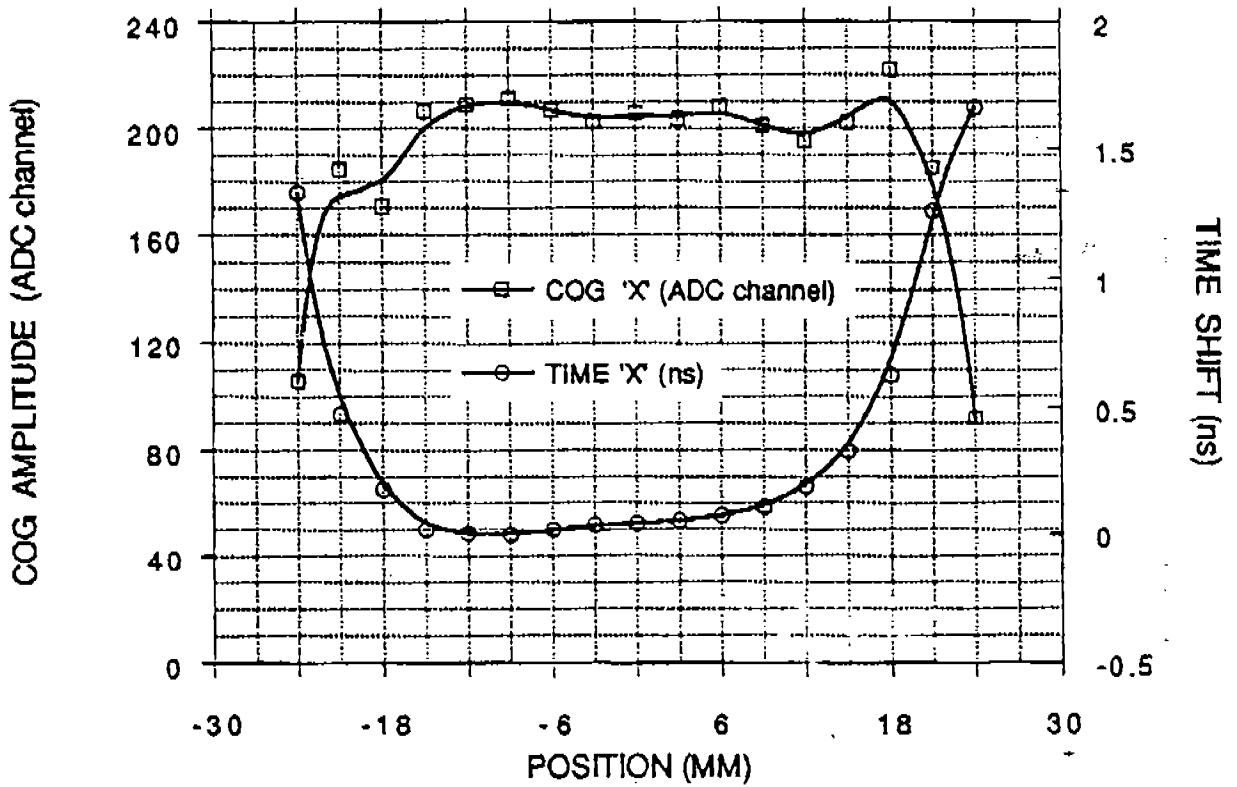


Figure 4: The transit time differences (right-hand vertical axis) of the photomultiplier as a function of distance from the cathode center along an axis 'x'. The plot represents real data measured at CEBAF.

EMI-9954A 'Y' SCAN AMPLITUDE & RELATIVE TIME SHIFT
 @ 2000 V

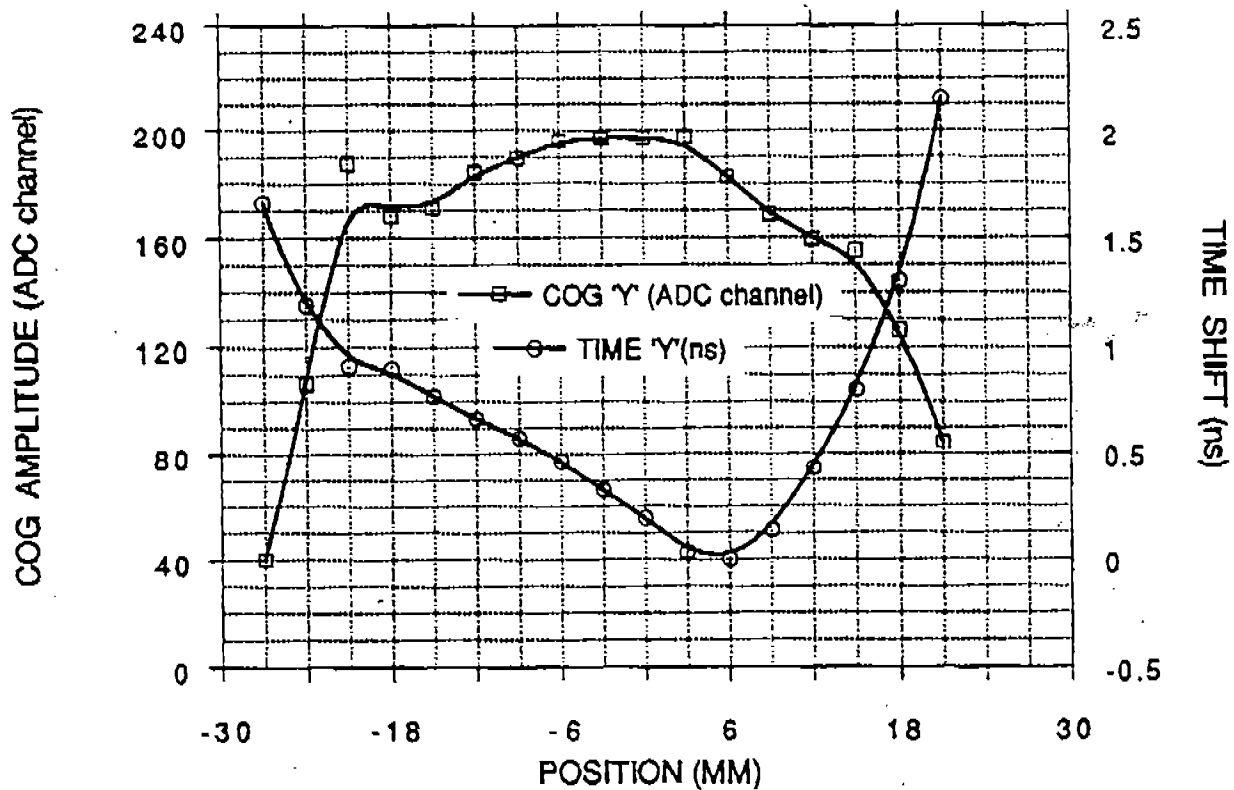


Figure 5: The transit time differences (right-hand vertical axis) of the photomultiplier as a function of distance from the cathode center along an axis 'y'. The plot represents real data measured at CEBAF.

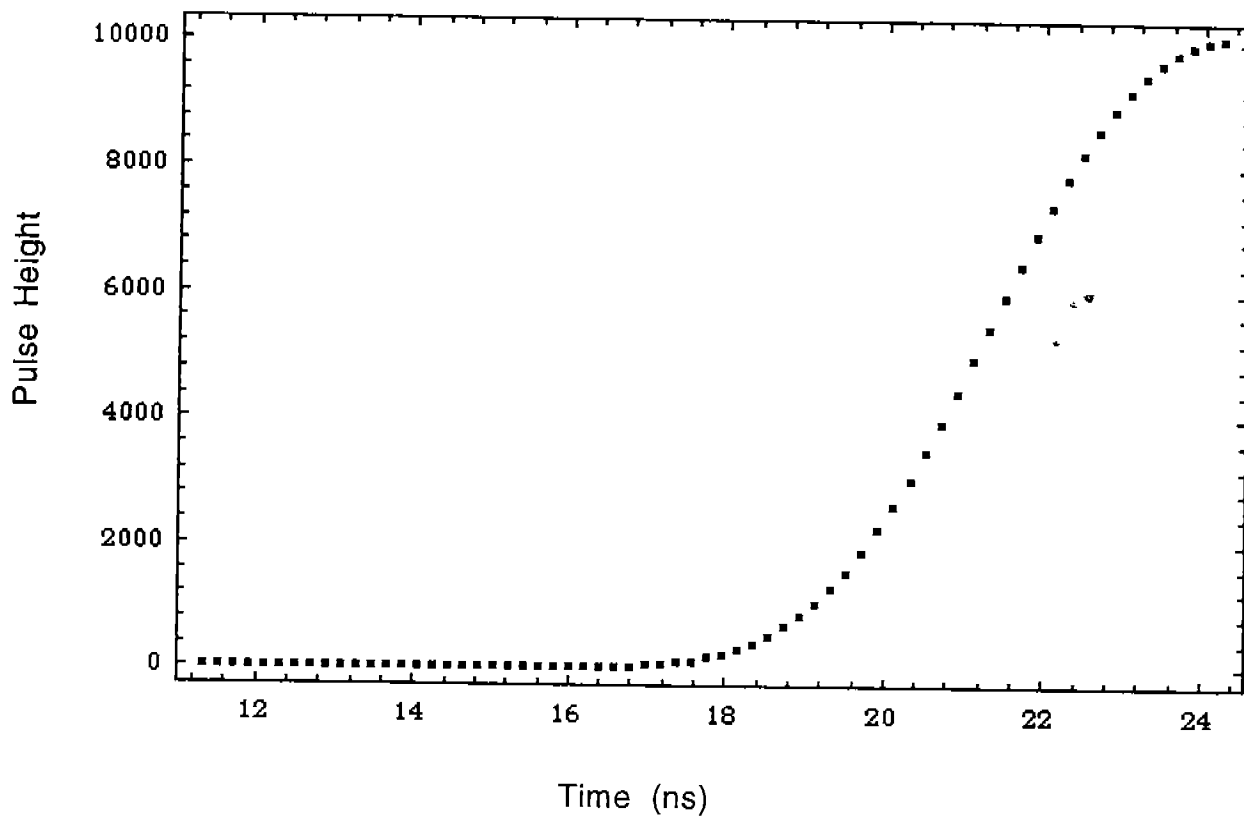


Figure 6: The array representation of the leading edge of a pulse as used in the Mathematica calculations. The pulse is from a source position of 172 cm into the scintillator and through the center and convoluted with a Gaussian with FWHM of 3.5 ns.

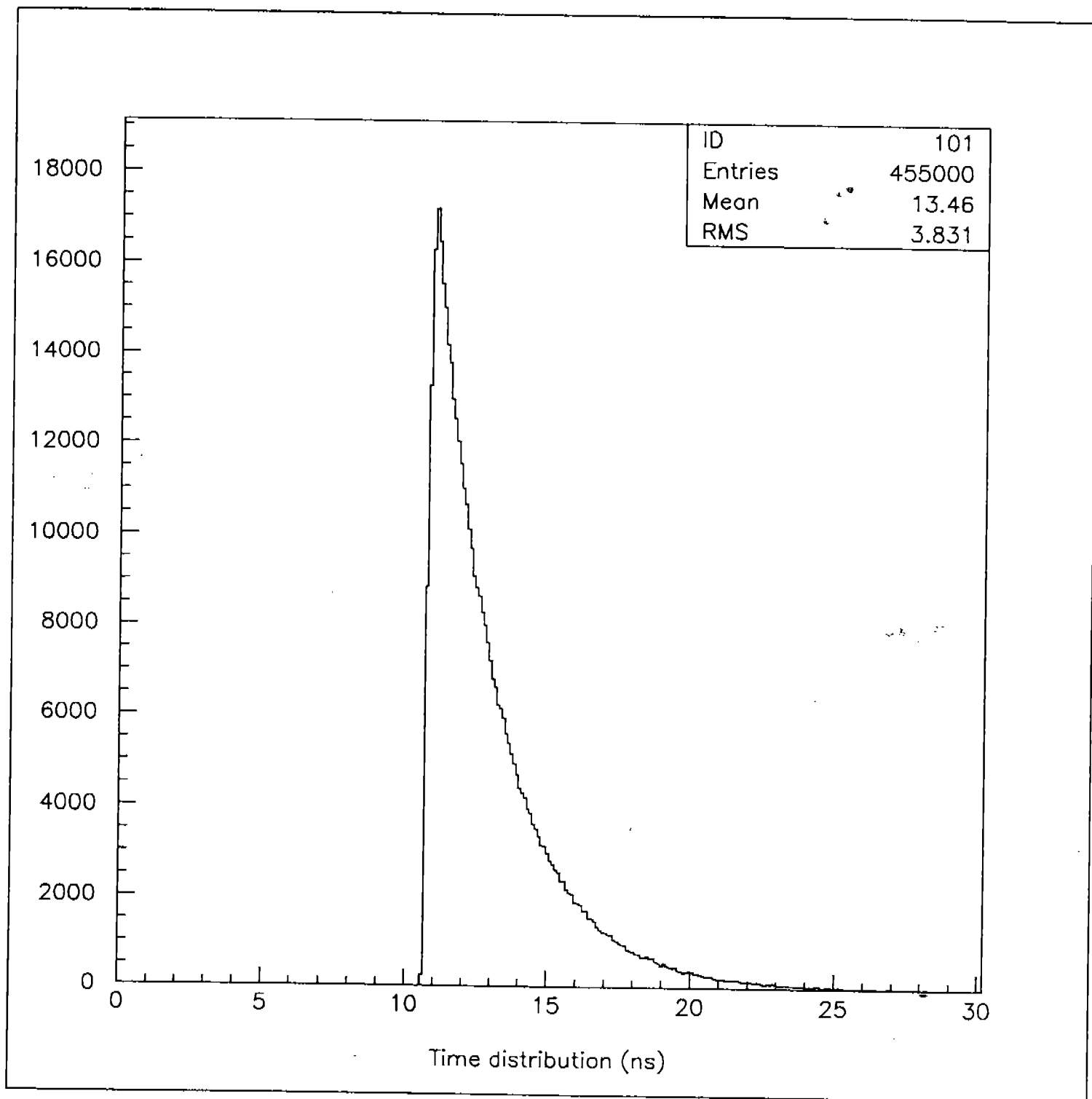


Figure 7: The pulse-histogram corresponding to a point light source in the center of the scintillator cross-section [(0,0) in Fig. 3] and at a distance of 0.1 cm into the scintillator end closest to the PMT

Edge (dash) and Center (solid) Path Photon Sources

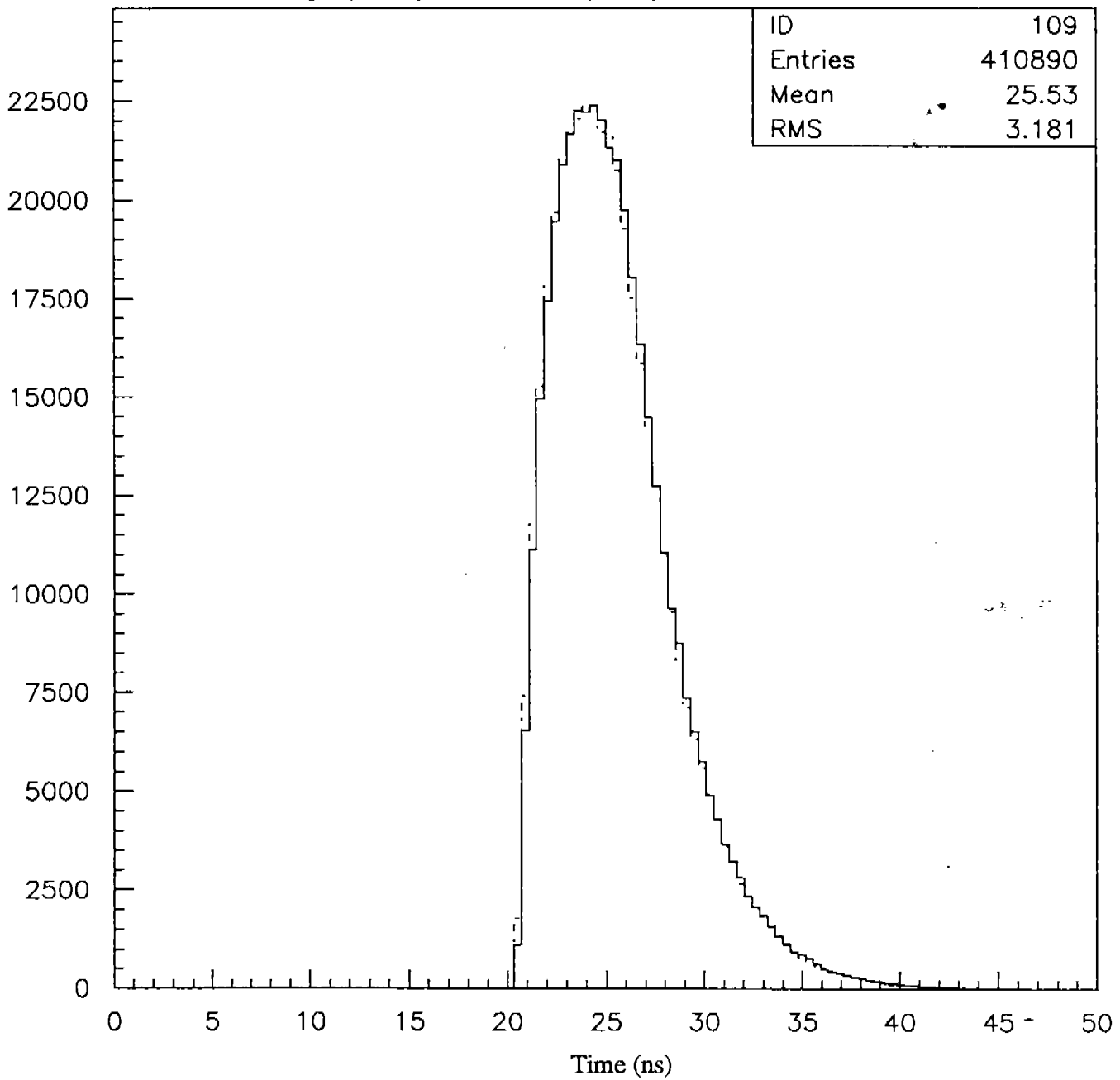


Figure 8: Overlaid histograms of unconvoluted (for clarity) pulses generated using the center (solid) and edge (dash) light source geometries at -172 cm.

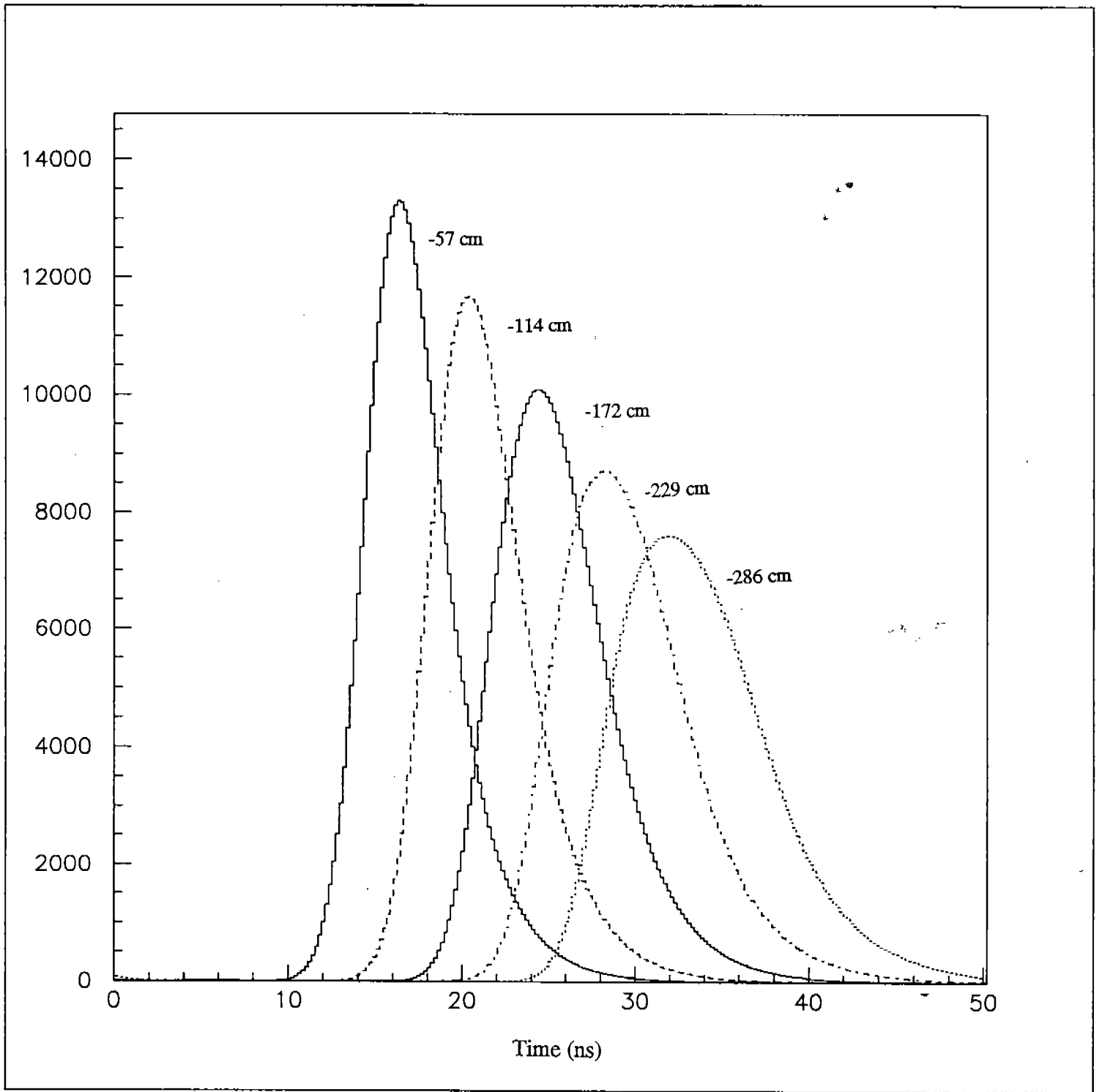


Figure 9: Overlaid histograms corresponding to pulses generated by center path light sources at various distances. From left to right, the light source path positions are -57 cm (solid), -114 cm (dash), -172 cm (solid), -229 cm (dash), -289 cm (dot).

Convolutions at 172cmz 2.5ns response (dash), 3.5ns (solid), 4.5ns (dot)

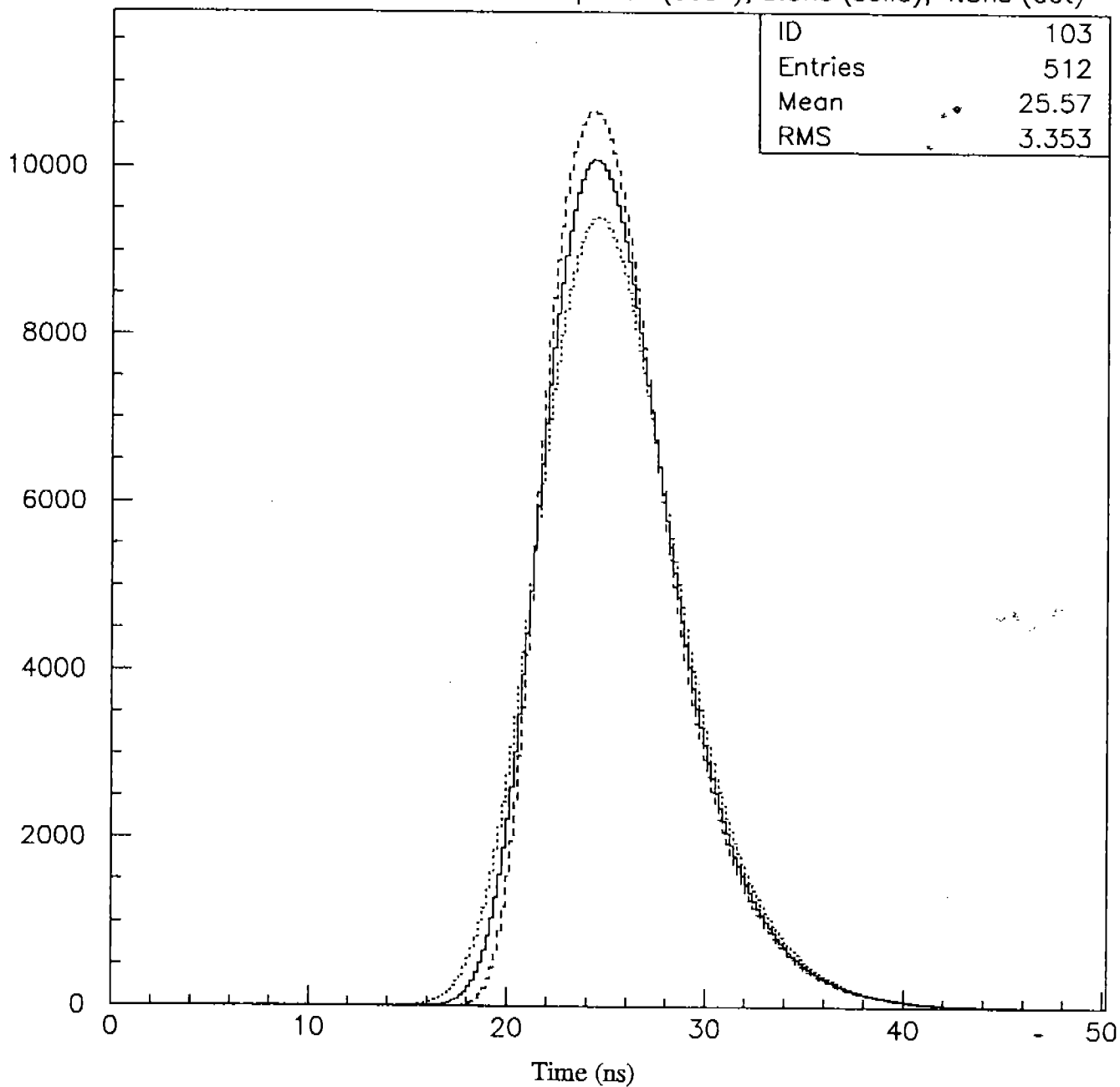


Figure 10: Overlaid histograms of pulses from a single center path light source at -172 cm convoluted by three different response functions of FWHMs: 2.5 ns (dash), 3.5 ns (solid), 4.5 ns (dot).

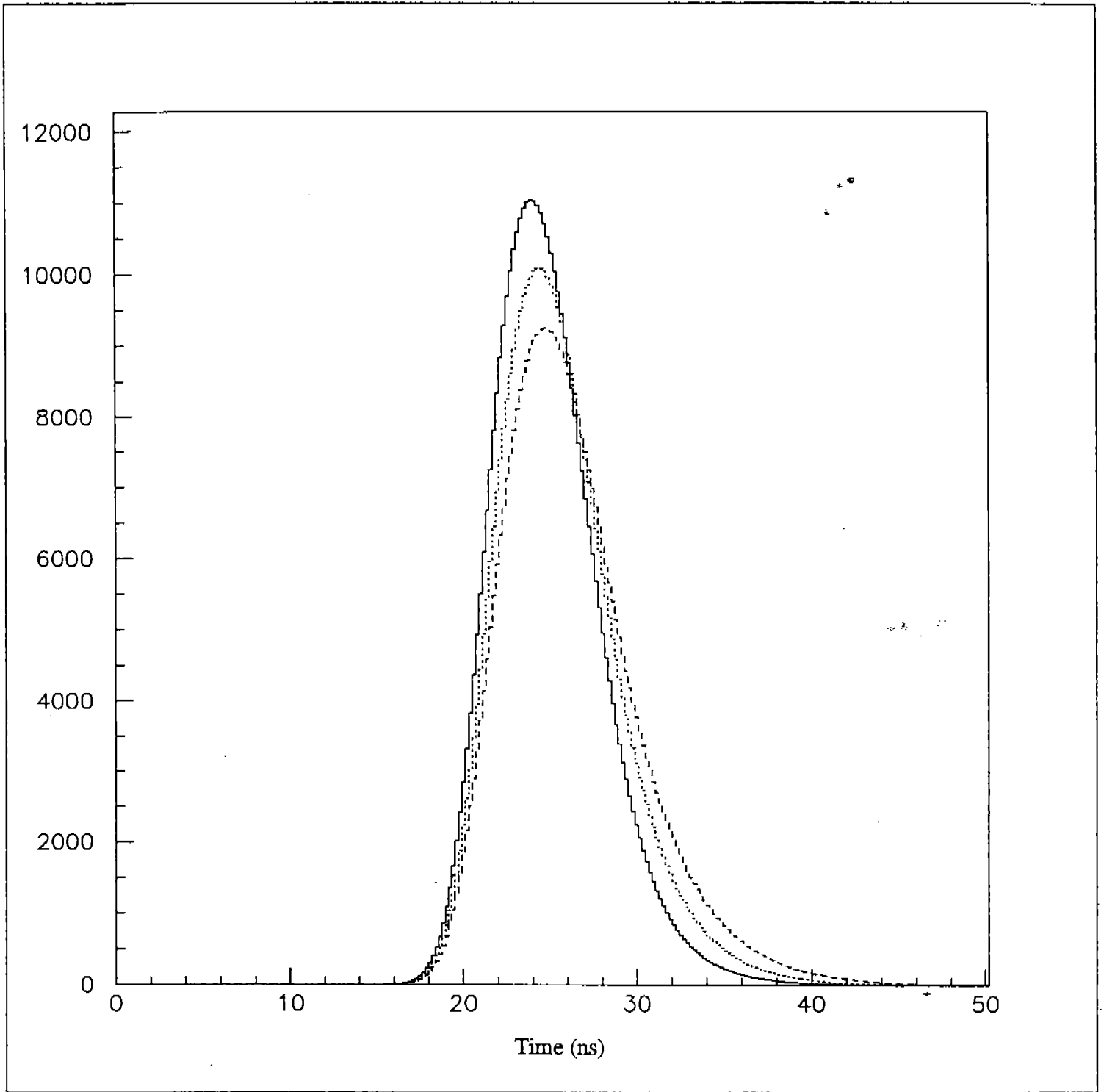


Figure 11: Overlaid histograms of pulses from center path light source at 172 cm using different scintillation decay time constants; 1.6 ns (solid), 2.3 ns (dot), 3.0 ns (dash).

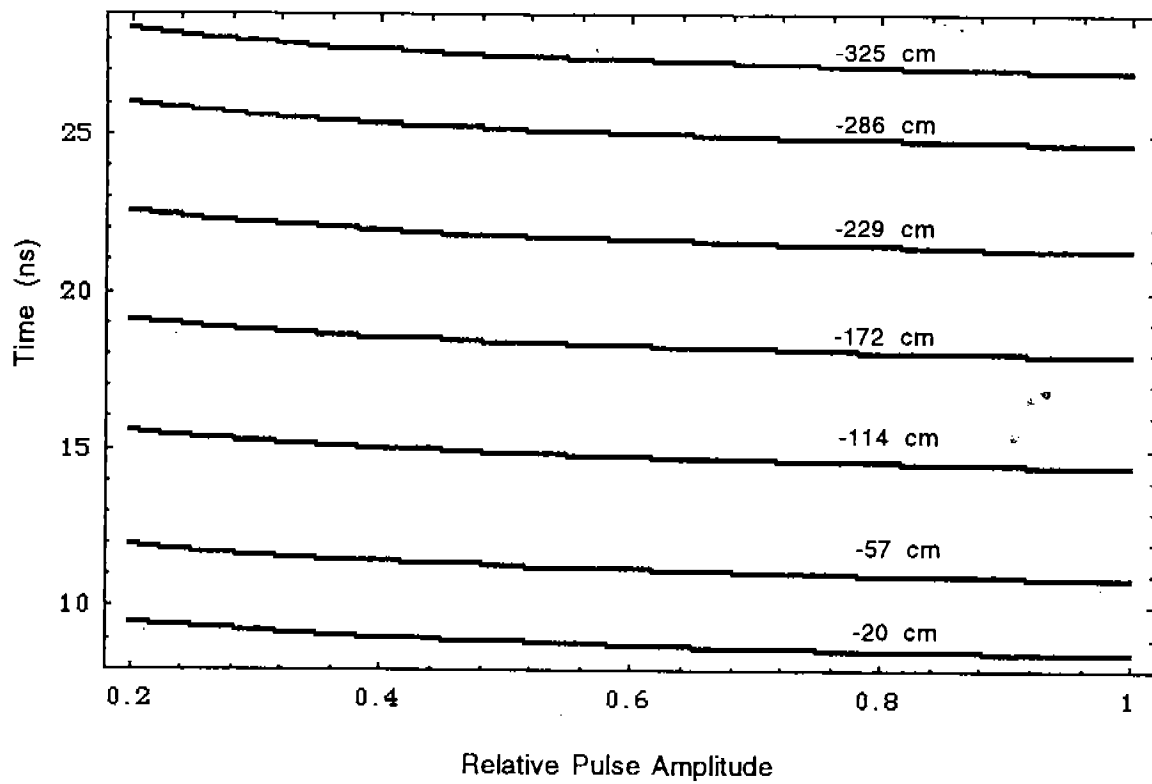


Figure 12: The time-walk curves for 7 points along the TOF scintillator: -20cm, -57cm, -114cm, -172cm, -229cm, -286cm, -325cm.

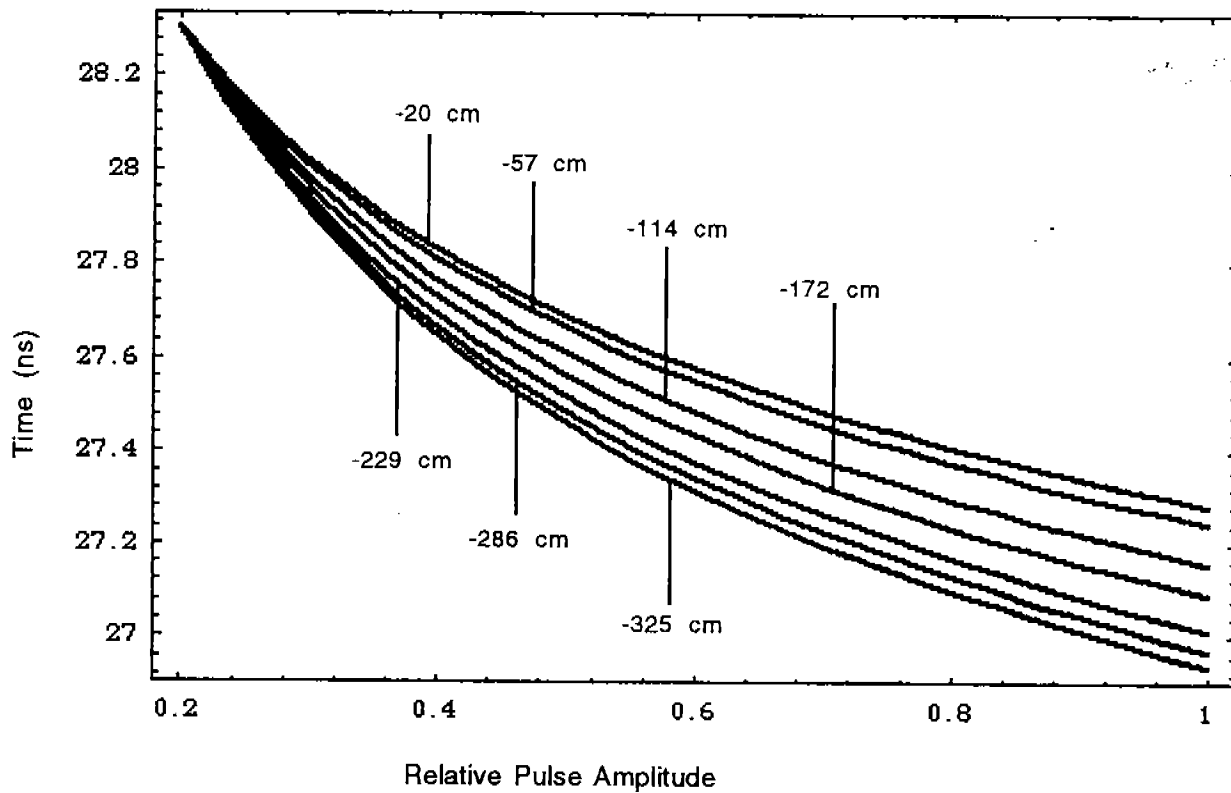


Figure 13: A vertically-adjusted presentation of time-walk plots corresponding to different source particle path distances from the end of the scintillator.

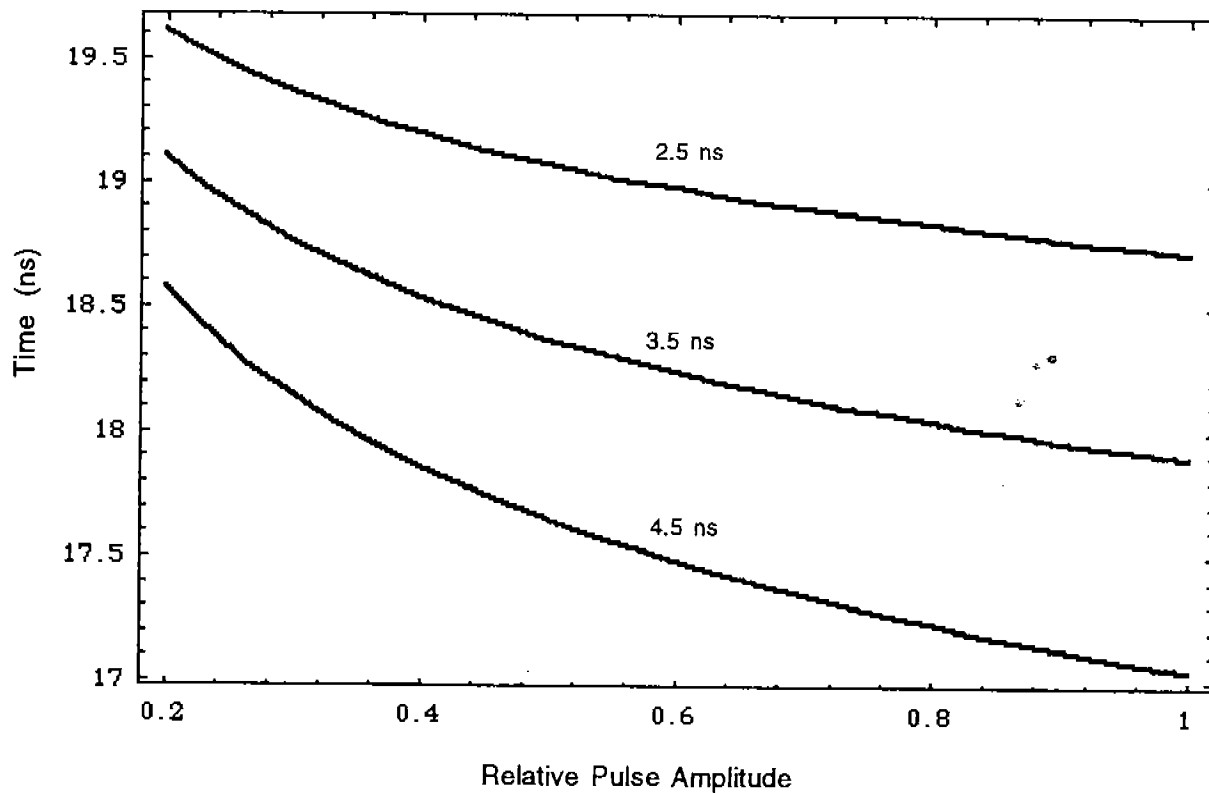


Figure 14: The time-walk curves for a pulse from a light source path at -172 cm through the center of the scintillator varying the convolution response function. Labeling each curve is the FWHM of the Gaussian response function used for convolution.

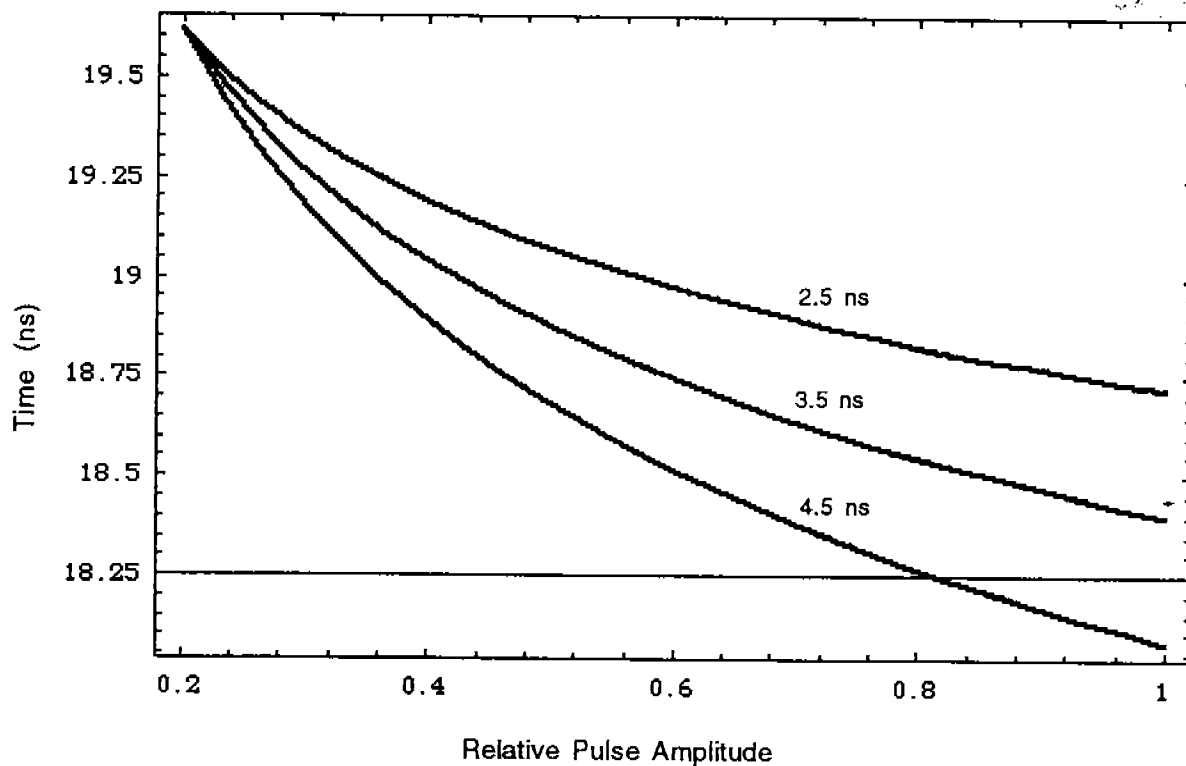


Figure 15: The vertically-adjusted time-walk curves for a pulse from a light source path at -172 cm through the center of the scintillator varying the convolution response function used. Labeling each curve is the FWHM of the Gaussian response function used for convolution.

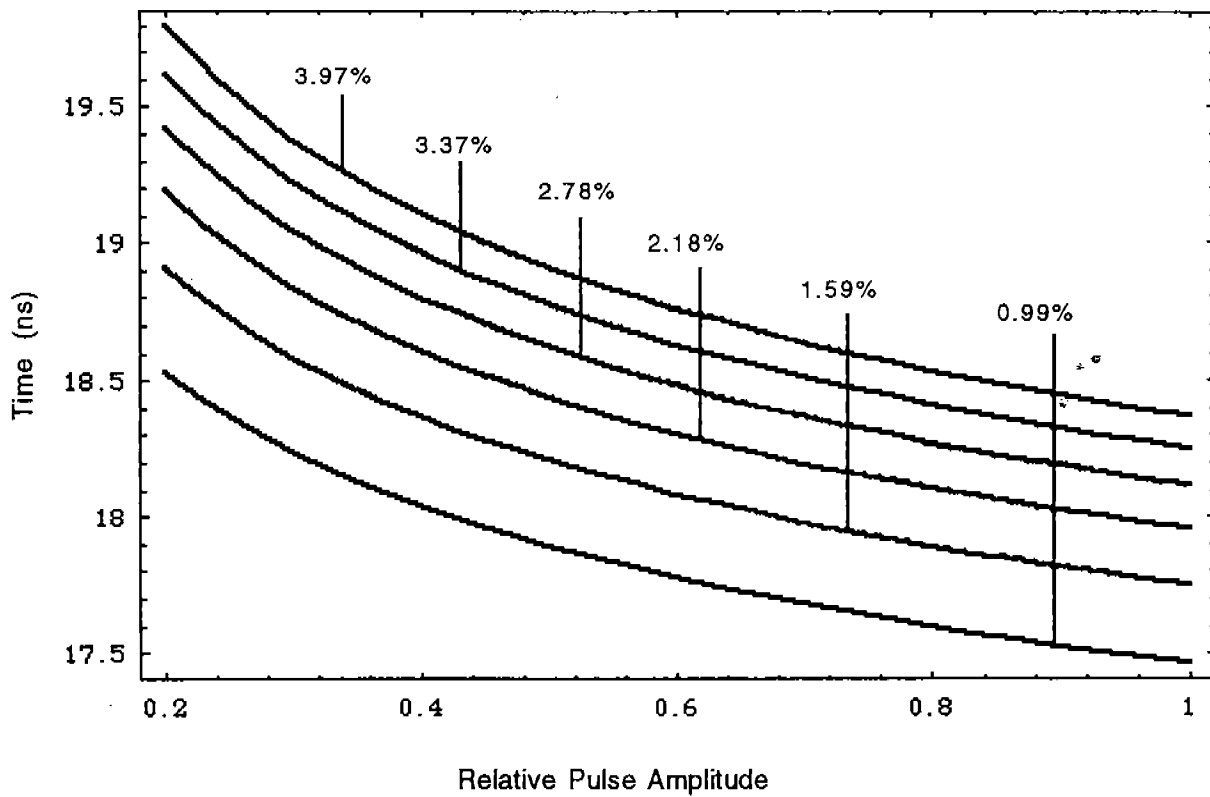


Figure 16: Time-walk plots for a pulse from a light source path at -172 cm, convoluted with a Gaussian of width 3.5 ns, using different discriminator thresholds in the time-walk calculation. The discriminator thresholds are here represented as percentages of the maximum pulse height.

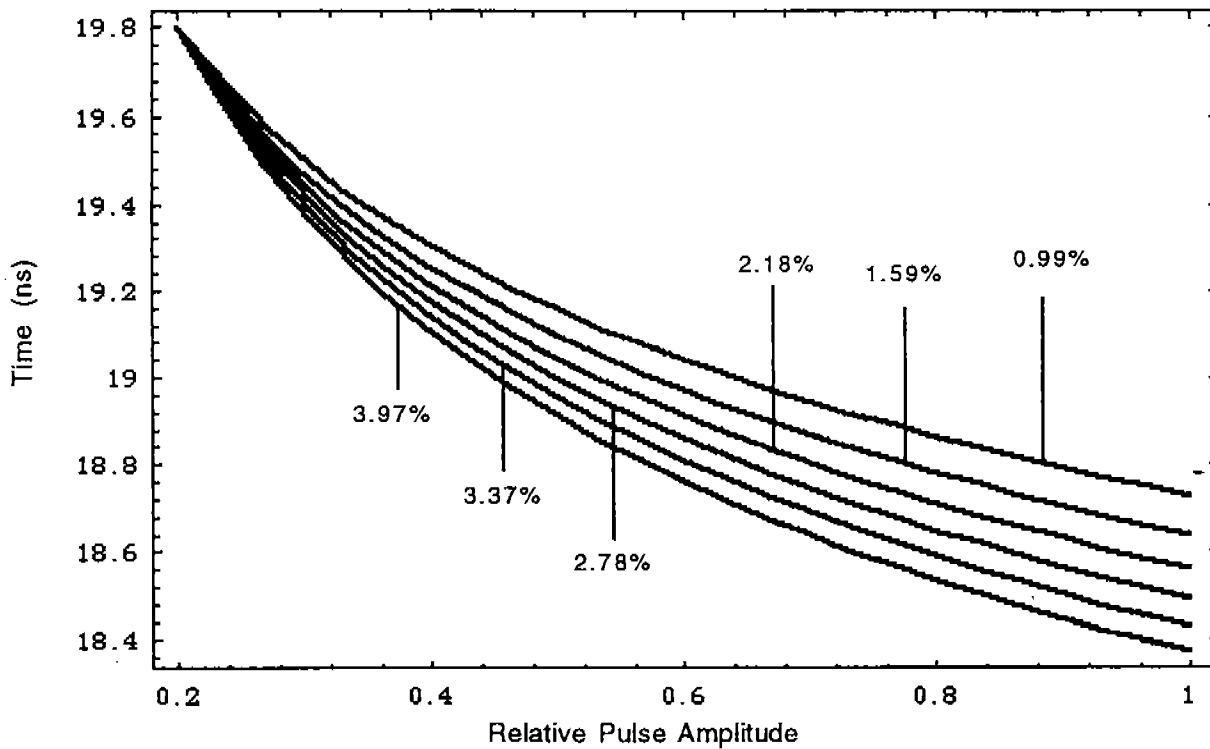


Figure 17: Time-walk plots for a pulse, vertically adjusted, from a light source path at -172 cm convoluted with a Gaussian of width 3.5 ns, using different discriminator thresholds in the time-walk calculation. The discriminator thresholds are here represented as percentages of the maximum pulse height.

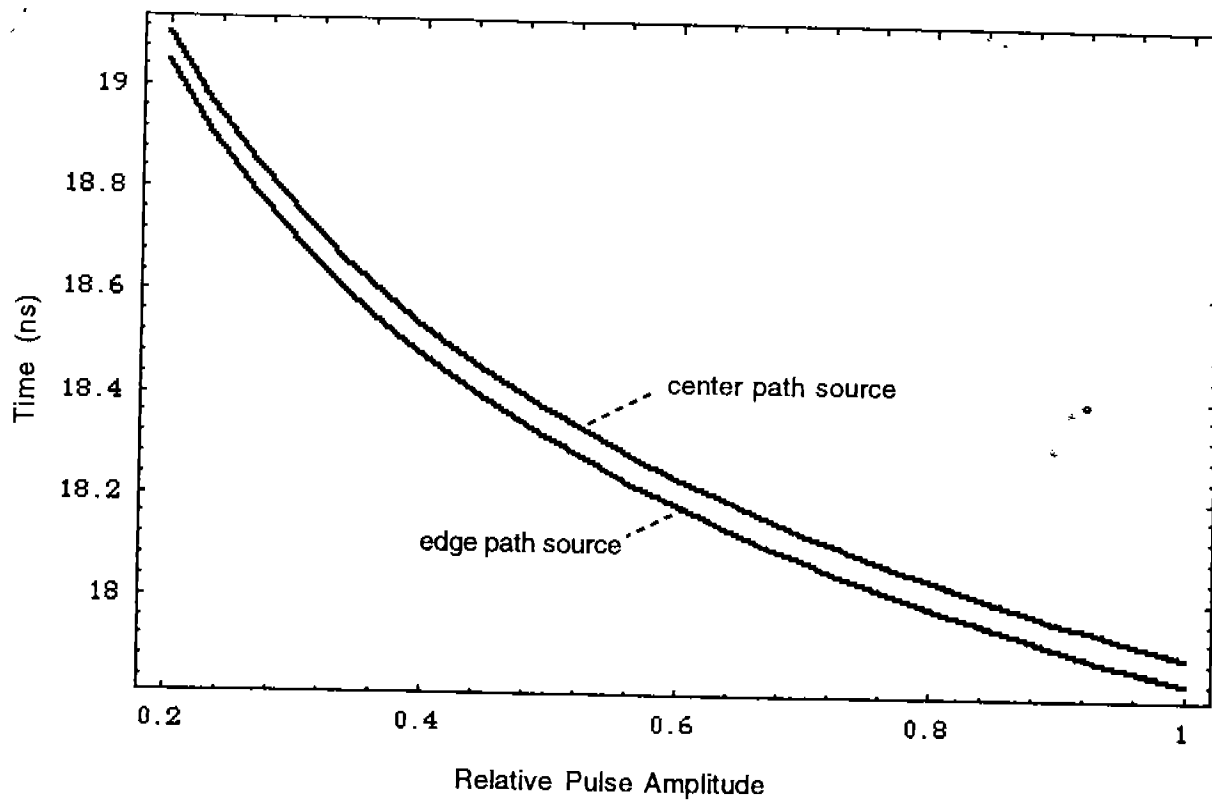


Figure 18: The time-walk plots for center and edge paths at -172 cm into the scintillator convoluted with a Gaussian of 3.5 ns width.

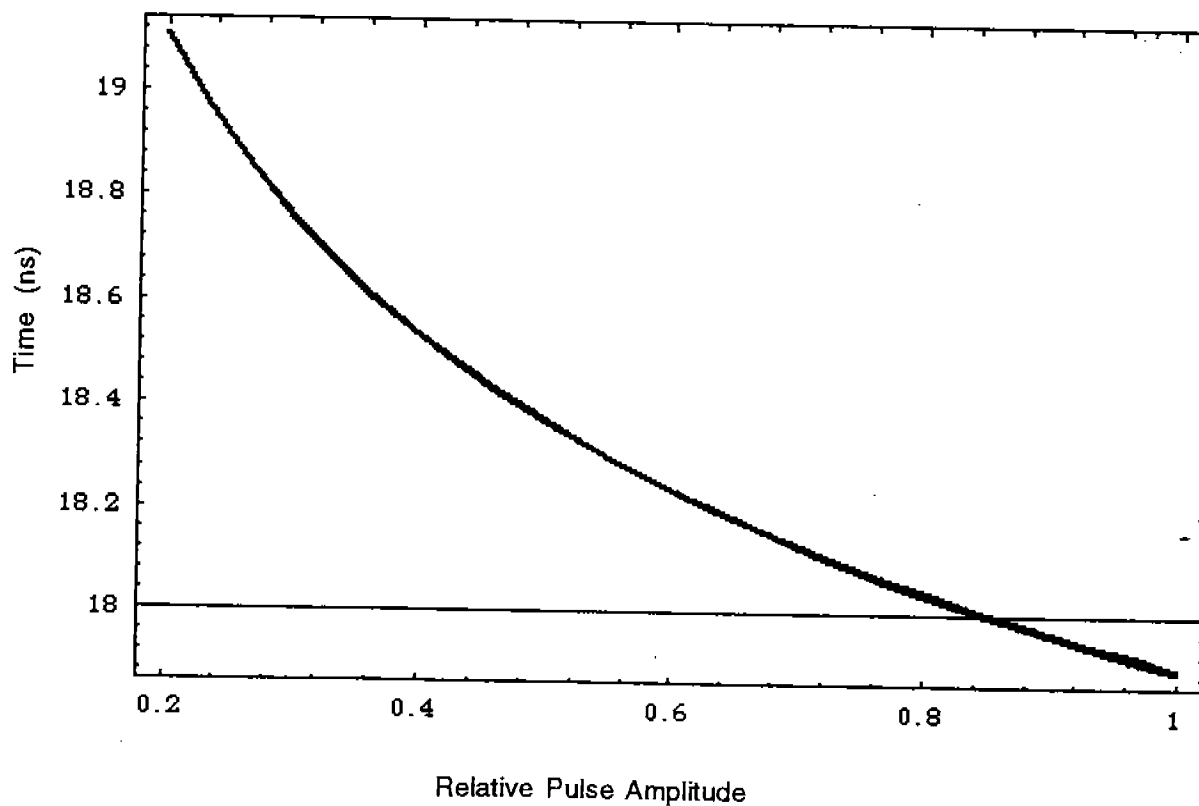


Figure 19: The respective time-walk, adjusted vertically, for center and edge paths at -172 cm into the scintillator convoluted with a Gaussian of 3.5 ns width.